



## Study the Effect of Gold Film Thickness on the Sensitivity of the U Shape Fiber Sensor by the Occurrence of LSPR Phenomenon

Saffana Z. Maseer<sup>1,\*</sup>, Bushra R. Mahdi<sup>2</sup>

*\*Corresponding author: saffana.zeiab1202a@ilps.uobaghdad.edu.iq.*

1. Institute of Laser for Postgraduate Studies, University of Baghdad, Iraq, Baghdad, Iraq.
2. Ministry of Science and Technology, Materials Research Department, Laser Center, Iraq, Baghdad.

(Received 4/7/2022; accepted 19/9/2022)

**Abstract:** In this paper, a U-shaped probe with a curvature diameter of half a centimeter was implemented using plastic optical fibers. A layer of the outer shell of the fibers was removed by polishing to a D-section. The sensor was tested by immersing it in a sodium chloride solution with variable refractive index depending on solution concentrations ranging from 1.333 to 1.363. In this design, the sensor experienced a decrease in its intensity as the concentration of the solution increased. The next step The sensor was coated with a thin layer of gold with a thickness of 20 nm, and the sensor was tested with the same solutions which resulted in a shift in wavelengths where the shift in wavelength was 5.37 nm and sensitivity 179 nm / RIU. To study the effect of the thickness of the film, it was coated with a second layer of gold to make the total thickness 30 nm. The results showed an improvement in the sensitivity with increasing the thickness of the coating, to become 466.66 nm / RIU and the wavelength shift was 14 nm.

**Keywords:** Plastic optical fiber, Gold NanoParticles, U Bend optical fiber, DC Plasma coating.

### 1. Introduction

Numerous fiber-optic sensing devices have been studied and created during the last two decades. [1]. Refractive index (RI) sensors, pH sensors, strain sensors, temperature sensors, curvature sensors, and humidity sensors are just a few of the sensing applications where optical fiber sensors have received significant attention [2],

Comparing fiber sensors to various traditional sensors, there are a number of benefits. Fiber sensors are small, light, have a high resolution, and good stability in addition to being immune to

electromagnetic interference and able to withstand high temperatures and radiation[3].

Due to their ease of handling and economic efficiency, plastic optical fibers (POF) manufactured of polymethylmethacrylate (PMMA) are receiving more attention as a viable replacement to silica-based fiber optic sensors, because POF is so flexible, any required fiber probe design such as tapered, side-polished, U-bent, coiled, or any other may be easily achieved to get a strong evanescent field at the core-cladding interference[4]. Nanotechnology's most recent advancements have resulted in new breakthroughs for localized surface Plasmon

resonance (LSPR) fiber optical sensors. The shape, size, substance, and refractive index of the surrounding medium all influence the extinction range generated by the LSPR phenomenon[5][6]. Due to their excellent optical properties, gold nanoparticles (Au-NPs), a sensitive coating among nanosized metallic materials, are frequently used in optical sensing applications[7]. By coating the optical fiber with a controlled layer of gold nanoparticles, a reliable LSPR-based sensor may be produced[8]. Because the coating thickness must always be less than the evanescent wave's penetration depth, controlling the coating thickness on a nanoscale scale is a crucial quality for sensors based on the interaction of the evanescent field with the coating. The evanescent wave absorbance heavily depends on the analytic concentrations, assuming no other variables change[7]. When the probes coated with gold layer with thickness greater than the evanescent wave penetration depth would not lose light on the sensing region since the film transmittance was negligible such that practically all the light would be reflected and remain inside the fiber, so that the thicker the layer, the smaller the sensitivity[9].

Side-polished fiber, tapered fiber, hetero-core structured fiber, and U-shaped fiber are just a few of the fiber configurations that have been suggested to increase the sensitivity of fiber SPR. The U-shaped fiber SPR sensor has been proven to be more sensitive than the traditional straight fiber SPR sensor[10]. Part of the light from the core mode is coupled into the cladding and generates numerous sets of higher-order modes as it passes from the straight portion of the sensor fiber into the U-bent area, the guided light rays in the sensing region reflecting at angles closer to the critical angle and more optical power is decayed into the sensing medium this enhances the light matter interaction and the sensitivity increases[11]. Although U-shaped fiber sensors significantly increases sensitivity, in most cases structural modification techniques like tapering by polishing

are employed to increase the sensitivity of optical fiber sensors. When the U-shaped outer curvature is removed by polishing, the evanescent field's power and penetration depth increase because when the outer curvature of the U-shaped POF is removed by polishing; the RI difference between the analytic and the inner curvature of fiber will decrease, leading to the increase of evanescent wave power, as well as its penetration depth. These structural modifications are used to improve the sensitivity better sensing performance is made possible by these structural changes[12]

The interplay of the evanescent field and the surface electron released by the Plasmon metal is the basis of the SPR sensor's working theory. An evanescent field is produced at the U-bent area of the fiber by a light wave that is propagating in its core[9]. When the evanescent field strikes the metallic surface, it produces a surface Plasmon wave (SPW), the SPW propagates along the metal-dielectric surface. If the frequency of the evanescent wave and surface Plasmon mode is matched, the excitation of surface Plasmon at metal/dielectric interface results in the transfer of energy from incident light to surface Plasmon when the energy of light photons perfectly matches the Plasmon's' energy level, which reduces the intensity of the output light[13]. Typically, the bend loss of U fiber sensor is comparable to the intensity modulation, which is easily impacted by the light source and the surrounding environment [14].

In this paper U shape plastic optical fiber sensor was built with 0.5 cm bending diameter and tested it with sodium chloride solutions with change in refractive index from 1.333 to 1.363 then coated it with 20 nm thickness of GNPs and retested with the same sodium solutions. Finally, coated the bare sensor with 30nm thickness of GNPs and tested it with same sodium solutions to study the effect of GNPs thickness on the sensitivity of the sensor.

## 2. Experiment Work:

Based on macro-bending fiber losses, U shape fiber sensor have been designed and constructed by using plastic optical fiber.

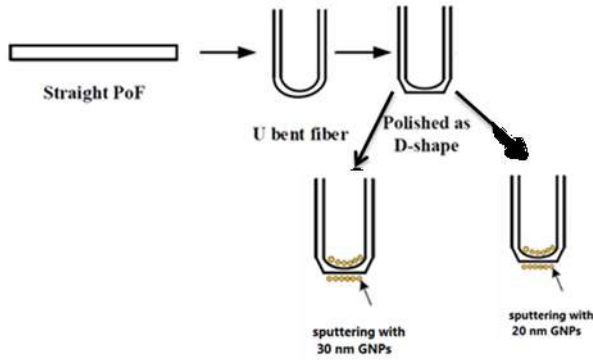


Figure1: steps of fabrication the sensor.

The steps of fabrication the sensor was shown in the figure 1.

Plastic optical fiber (POF) with 930  $\mu\text{m}$  diameter was made of PMMA with refractive indices 1.49 and 1.41 for core and cladding respectively was used as shown in figure2.

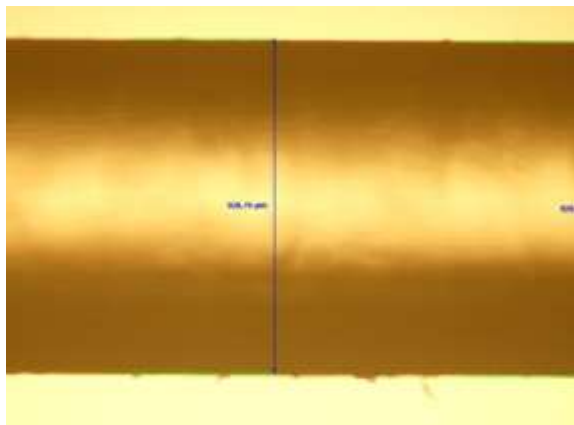


Figure2: straight Plastic Optical Fiber.

First, Straight Plastic optical fiber was bent in U shape handily with 0.5 cm bending diameter, the

sensors were installed on a plastic graduated ruler and secured with thermal adhesive.

The U-bent POF head sensor is polished using grinding papers to make it resemble a D shape in cross section, as shown in figure3(a). To ensure polishing perfection, the POF must be rigidly fixed. The upper portion of POF was mostly removed to roughly construct the appropriate probe profile using a rough polishing paper with bigger particles. The roughness of the exposed area was then further reduced using fine emery paper with finer particles, as can be seen in Figure3b

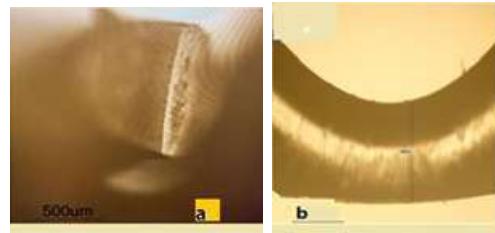


Figure 3: (a) Microscope image of the cross-section of the sensor tip from which the clad part has been removed and shown shape D. (b) Microscope image of polished POF, bent U-shape, fiber diameter after polishing 680  $\mu\text{m}$ .

Finally, GNPs sputtered on the head sensor by using DC Plasma coating device. The deposition rate of the coating layer was 20nm/hour. DC scattered plasma technology, a vacuum coating process classified under Physical Vapor Deposition (PVD) systems and primarily used for the deposition of metal alloys, composite textiles and other materials. The gold target represents the cathode electrode (The gold target with a thickness of (1 mm) a diameter of (5 cm), and a purity of (99.9%)), followed by a Teflon ring to fix the samples to be coated, as shown in Figure 4a, and the parts of the complete system are shown in Figure 4b where sensors are mechanically fixed on the Teflon ring, which is stable in the vacuum chamber between the cathode (gold target) and the

anode, obtaining a coating film thickness of 20 nm.

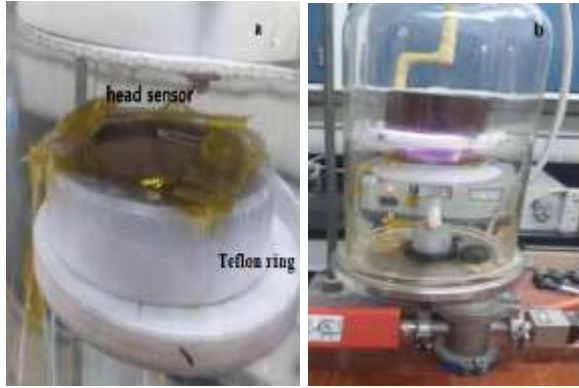


Figure 4: The demonstration system of DC Plasma coating device.

Figure 5 shows the sensor without coating in A and by coating a first layer with a thickness of 20 nm in (b) and a thickness of 30 nm in (c).

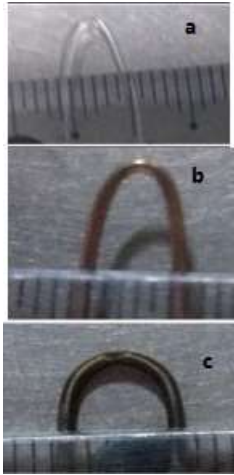


Figure5: (a) bare POF with 0.5cm bending diameter. (b) POF with 0.5cm bending diameter was coated with 20nm thickness of GNPs. (c) POF with 0.5cm bending diameter was coated with 30nm thickness of GNPs.

The coated fibers were examined under an electron microscope to test the size of the gold particles, which are shown in Figure 6, with two different scales of the SEM microscope.

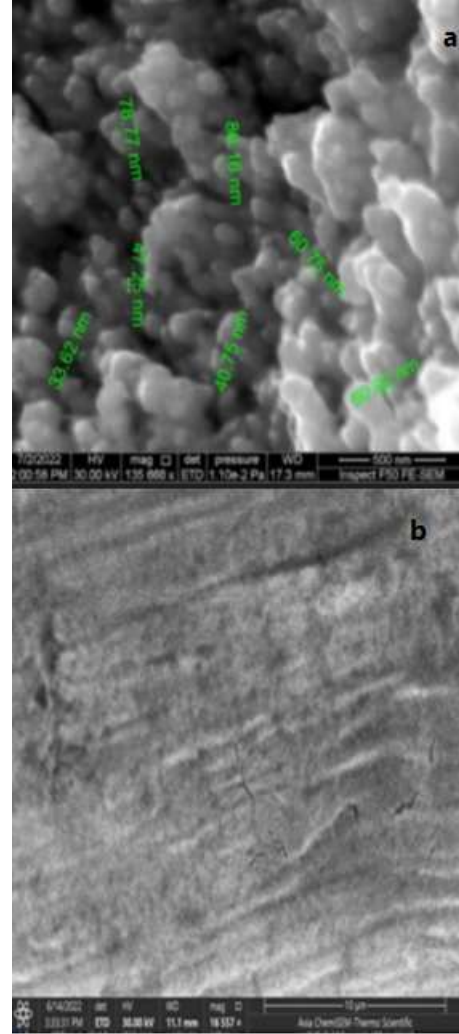


Figure 6: SEM (Scanning electron microscopy) image for GNPs in two scales (a) 500nm and (b) 10µm.

## 2.2 Experimental Setup:

In this experiment Semiconductor Laser with 650 nm and 5 mW was used as a source and Ocean 2000 was used as a spectrometer to record the laser beam transmitted on the computer as shown in figure 7.

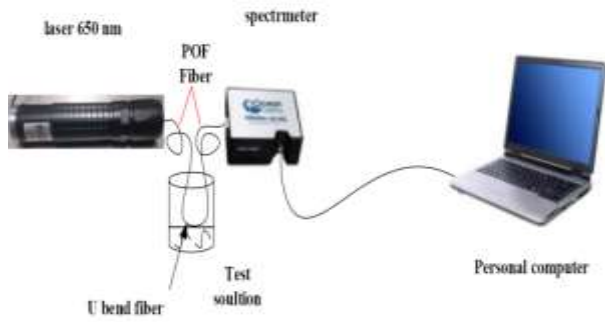


Figure 7: experimental setup.

### 2.3 Refractive Index solutions:

Sodium chloride solutions with different concentrations are used as samples with different RIs. NaCl solutions were prepared by taken different concentration values of the Salt powder dissolved in distal water at room temperature. Abbe refractometer measured the refractive index of the solutions with ranges (1.333-1.363).

Table 1: The refractive indices of the sodium chloride solutions.

RI	Abbreviation	Concentration
1.333	Distal water	0
1.339	C1	1mg/ ml
1.342	C2	2 mg/ml
1.350	C3	3 mg/ml
1.358	C4	4 mg/ml
1.363	C5	5 mg/ml

### 3. Result and Discussion:

Intensity counts (number of photons that the spectrometer was detected it) was recorded to characterize the NaCl solutions for U bent POF sensor with 0.5 cm bending diameter without coating.

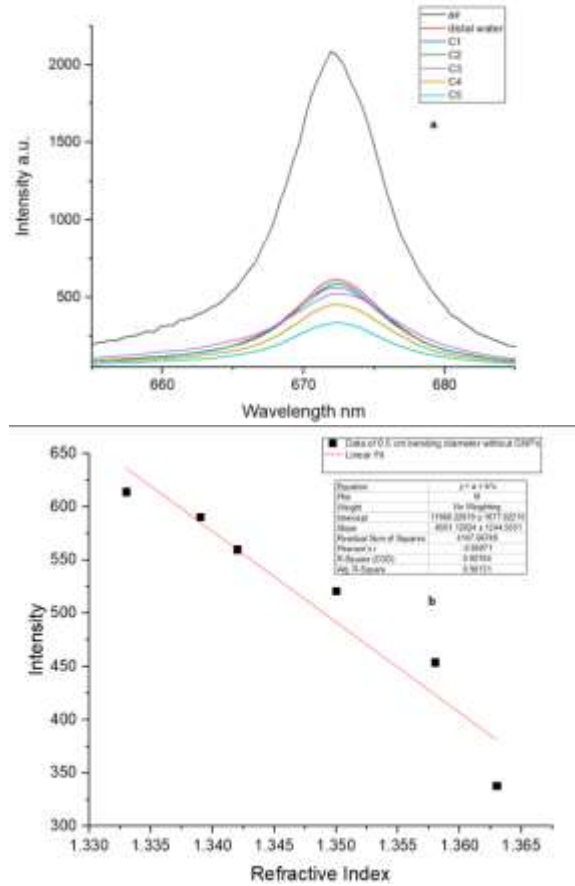


Figure 8: (a) Response of U shape bare POF sensor with 0.5 cm bending diameter to refractive index change. (b) Linear fit between Intensity and refractive index change.

It is noted in figure 8 a that the intensity spectrum of sodium chloride solution with different concentrations and refractive indices ranges from 1.333 to 1.363, where there is no shift of wavelengths, but the intensity decreases with the increase in the concentration of the solutions this occurs because the increased concentration of chloride sodium solution increases absorption of light power by the solution resulting in decreasing in the intensity of light. The sensitivity of change the Intensity with refractive index change was  $-8501\Delta I/RIU$  ( $\Delta I/RIU$  change in intensity per refractive index change) for this sensor was calculated from the linear fit in figure 8(b).

Then LSPR wavelengths were recorded to characterize the NaCl solution for U shape POF sensor with 0.5 cm bending diameter with 20nm thickness of GNPs shown in figure 9 and U bent POF with 30nm thickness of GNPs shown in figure 10.

It is evident from figure 9 (a) that as the concentration of NaCl solution increase the LSPR wavelength gradually move to longer wavelength ( $\Delta\lambda=5.37$ ) with peak intensity decreasing. figure 9c show the linearity between the LSPR wavelength and the refractive index change the sensor response was showed to be linear with  $R^2= 0.96$  and the sensitivity of LSPR wavelength with refractive index change was 179 nm/RIU.

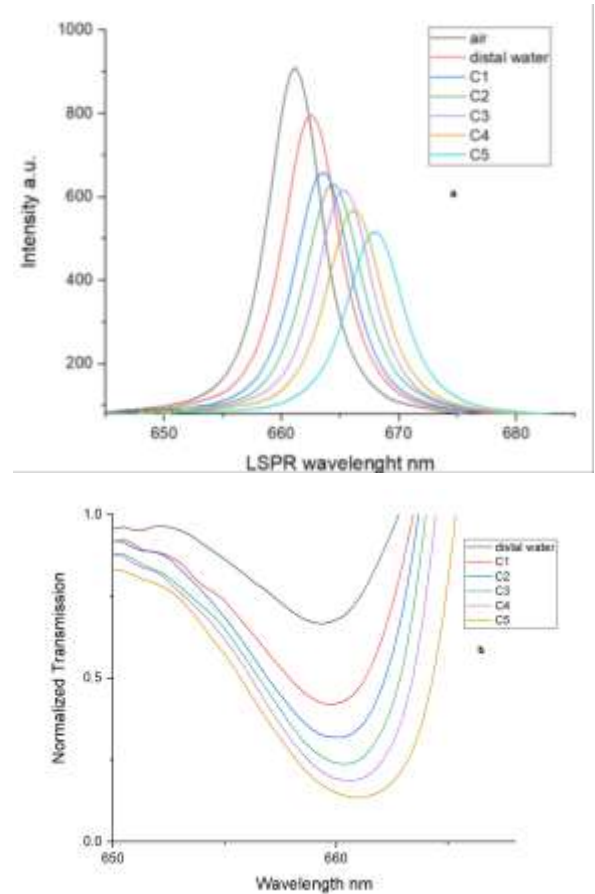
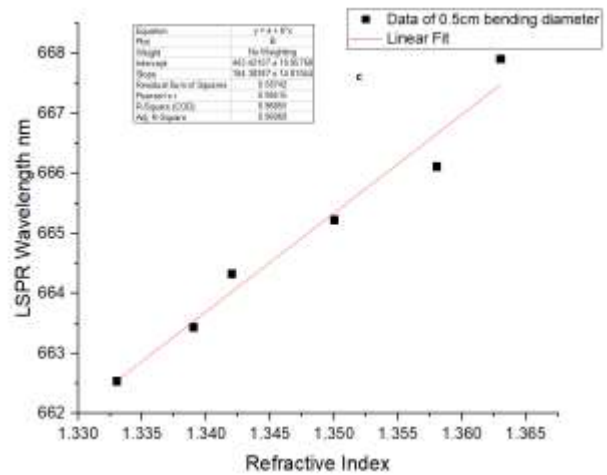


Figure 9: (a)



Response of U shape POF sensor with 0.5 cm bending diameter with 20 nm GNPs thickness. (b) Normalized Transmission spectrum. (c) Linear fitting curve.



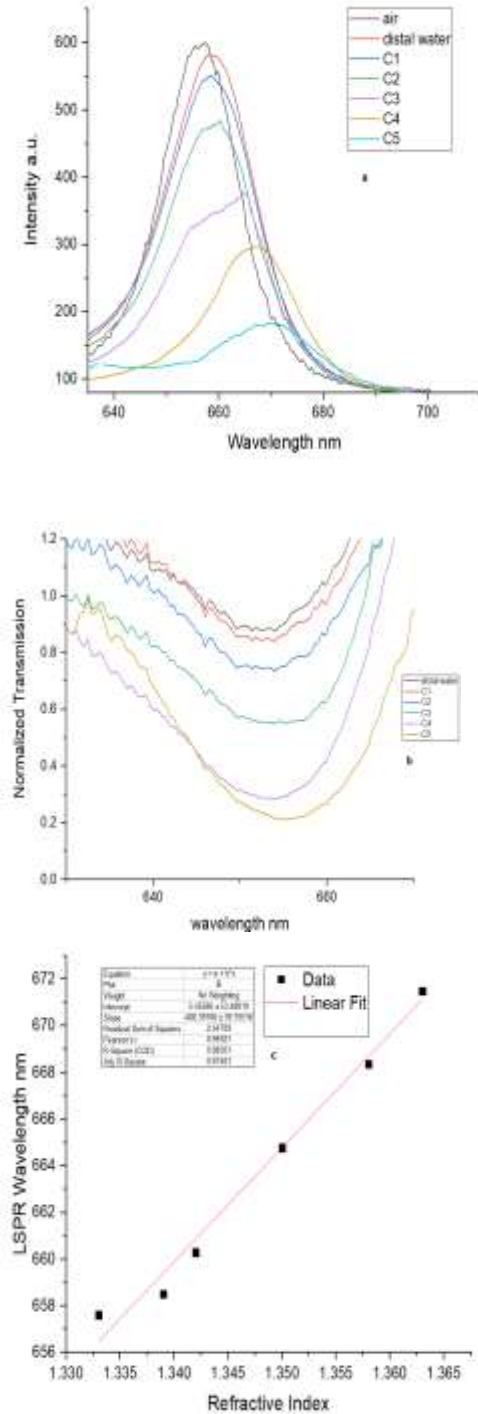


Figure10: (a) The response intensity of U shape sensor with 0.5 cm bend diameter coated with 30 nm thickness of GNPs immersed in different concentrations of NaCl solution. (b) Normalized transmission. (c) Linear Fitting curve.

It can be observed in figure 10a that 14 nm red shift of LSPR wavelength with increase the sodium chloride solution concentrations at room temperature, the red shift of the local resonance wavelength get larger due to addition more thickness of GNPs. In figure 10 c the sensor response to refractive index change was found to be linear with  $R^2=0.98$  and higher sensitivity of 466.66 nm/RIU was obtained. This occurs because the increase in GNPs thickness allows more significant interaction between surface Plasmon mode and fiber mode that giving an SPR resonant wavelength more shift[4] [15]. These findings is agreement with results of the study in reference[16], [4] and [10] (For various RI solutions, the probes with increased film thickness show strong SPR wavelength sensitivity).

The change in resonance wave length with change in refractive index of sensing media can explain by the principles of SPR and the intensity decreasing occurs because the increased concentration of outside solution increases absorption of light power by the solution resulting in decreasing in the intensity of light because U bent sensor based on Intensity modulation.

The normalized transmission curves that shown in figures 9b and 10 b that the higher concentration of the solution, the greater depth of the transmittance curves with red wavelength shift because the LSPR phenomena was occurred. Normalized transmission curves were calculated from transmittance equation:  $T = \frac{I_{out}}{I_{in}}$

Transmittance is unit less. Where  $I_{in}$  is the reading of intensity for air,  $I_{out}$  is the reading of intensity for solutions.

**Table (1): Comparing the sensitivity between some optical LSPR sensors.**

Sensor type	Material	sensitivity nm/RIU	Reference
D shape fiber	GNPs	580	[17]
U bent fiber	MoS2 -gold film	6184.4	[18]
U bent fiber	Gold nanoparticles	466.66	This work

#### 4. Conclusion:

In this study, a U-shaped fiber-optic sensor was built using a plastic optical fiber with a curvature diameter of 0.5 cm, and part of the fiber's outer cortex was removed in the bending region to become a D-shape. This sensor was tested on sodium chloride solution with refractive index change from 1.333-1.363 and it was noted that the wavelengths do not shift, but the intensity decreases with increasing concentrations of the sodium chloride solution. When the sensor was coated with gold nanoparticles with a thickness of 20 nm, a red shift of wavelengths was observed by 5.12 nm with an increase in the concentration of sodium chloride solution and 179 nm/RIU obtained sensitivity, for coating the sensor with 30 nm thick gold nanoparticles, a wavelength shift of 14nm was observed with increasing concentrations of sodium chloride solution and a higher sensitivity of 466.66 nm/RIU was obtained. The coating with GNPs enhanced the sensitivity for the sensor. This sensor is simple, has good detection specificity and excellent reliability, it can be used in bio/chemical applications.

#### References:

- [1] M. M. Hasan and H. J. Taher, "The Influence of No-Core Fiber Length on the Sensitivity in Fiber Optic Strain Sensor," *Iraqi J. Laser*, vol. 20, no. 1, 2021.
- [2] S. L. Kashen and H. J. Taher, "The influence of no-core fibre length on the sensitivity Optical fibre Humidity sensor," *Iraqi J. Laser*, vol. 20, no. 2, pp. 18–23, 2021.
- [3] S.-K. Liaw, "Introductory Chapter: An Overview the Methodologies and Applications of Fiber Optic Sensing," *Fiber Opt. Sensing-Principle, Meas. Appl.*, 2019.
- [4] C. Christopher, A. Subrahmanyam, and V. V. R. Sai, "Gold Sputtered U-Bent Plastic Optical Fiber Probes as SPR- and LSPR-Based Compact Plasmonic Sensors," *Plasmonics*, vol. 13, no. 2, pp. 493–502, 2018, doi: 10.1007/s11468-017-0535-z.
- [5] M. S. Sada, B. R. Mahdi, H. Ali, N. A. Aljbar, and M. A. Mohammed, "Localized surface plasmon resonance based photonic crystal fiber for cadmium detection," *NeuroQuantology*, vol. 19, no. 7, pp. 187–195, 2021, doi: 10.14704/nq.2021.19.7.NQ21102.
- [6] H. Song, H. Zhang, Z. Sun, Z. Ren, X. Yang, and Q. Wang, "Triangular silver nanoparticle U-bent fiber sensor based on localized surface plasmon resonance," *AIP Adv.*, vol. 9, no. 8, 2019, doi: 10.1063/1.5111820.
- [7] S. K. Al-Hayali, A. M. Salman, and A. H. Al-Janabi, "High sensitivity balloon-like interferometric optical fiber humidity sensor based on tuning gold nanoparticles coating thickness," *Meas. J. Int. Meas. Confed.*, vol. 170, p. 108703, 2021, doi: 10.1016/j.measurement.2020.108703.
- [8] M. H. Tu, T. Sun, and K. T. V Grattan, "Optimization of gold-nanoparticle-based optical fibre surface plasmon resonance (SPR)-based sensors," *Sensors Actuators B Chem.*, vol. 164, no. 1, pp. 43–53, 2012.
- [9] A. da S. Arcas, F. da S. Dutra, R. C. S. B. Allil, and M. M. Werneck, "Surface plasmon resonance and bending loss-based U-shaped



- plastic optical fiber biosensors,” *Sensors*, vol. 18, no. 2, p. 648, 2018.
- [10] T. Xie, Y. He, Y. Yang, H. Zhang, and Y. Xu, “Highly Sensitive Surface Plasmon Resonance Sensor Based on Graphene-Coated U-shaped Fiber,” *Plasmonics*, vol. 16, no. 1, pp. 205–213, 2021, doi: 10.1007/s11468-020-01264-x.
- [11] A. J. Y. Tan, S. M. Ng, P. R. Stoddart, and H. S. Chua, “Theoretical model and design considerations of U-shaped fiber optic sensors: A review,” *IEEE Sens. J.*, vol. 20, no. 24, pp. 14578–14589, 2020.
- [12] S. Wang, D. Zhang, Y. Xu, S. Sun, and X. Sun, “Refractive index sensor based on double side-polished u-shaped plastic optical fiber,” *Sensors (Switzerland)*, vol. 20, no. 18, pp. 1–13, 2020, doi: 10.3390/s20185253.
- [13] N. J. de Mol and M. J. E. Fischer, “Surface Plasmon Resonance: Methods and Protocols,” *Life Sci.*, p. 255, 2010, doi: 10.1007/978-1-60761-670-2.
- [14] B. Gholamzadeh and H. Nabovati, “Gholamzadeh e Nabovati - 2008 - Fiber Optic Sensors,” vol. 2, no. 6, pp. 1107–1117, 2008.
- [15] M. Iga, A. Seki, and K. Watanabe, “Gold thickness dependence of SPR-based hetero-core structured optical fiber sensor,” *Sensors Actuators, B Chem.*, vol. 106, no. 1 SPEC. ISS., pp. 363–368, 2005, doi: 10.1016/j.snb.2004.08.017.
- [16] J. Satija, N. S. Punjabi, V. V. R. Sai, and S. Mukherji, “Optimal design for U-bent fiber-optic LSPR sensor probes,” *Plasmonics*, vol. 9, no. 2, pp. 251–260, 2014, doi: 10.1007/s11468-013-9618-7.
- [17] N. Cennamo *et al.*, “Localized surface plasmon resonance with five-branched gold nanostars in a plastic optical fiber for biochemical sensor implementation,” *Sensors (Switzerland)*, vol. 13, no. 11, pp. 14676–14686, 2013, doi: 10.3390/s131114676.
- [18] H. Song, Q. Wang, and W.-M. Zhao, “A novel SPR sensor sensitivity-enhancing method for immunoassay by inserting MoS<sub>2</sub> nanosheets between metal film and fiber,” *Opt. Lasers Eng.*, vol. 132, p. 106135, 2020.

## دراسة تأثير سمك طلاء الذهب على حساسية مستشعر الليف البصري بشكل U على ظاهرة تردد الرنين السطحي الموقعي

سفانة ذياب مسير، بشرى رزوقي مهدي

معهد الليزر للدراسات العليا، جامعة بغداد، بغداد، العراق

الملخص: في هذا البحث، تم تصميم وتنفيذ متحسس الليف بصري المعتمد على ظاهرة رنين البلازمون السطحي الموقعي حيث تم تصنيع المتحسس باستخدام ليف بصري بلاستيكي وتم عمل انحناء له على شكل U بقطر انحناء مقداره 0,5 سم. ثم عمل صقل لراس المتحسس عند منطقة الانحناء ليكون شكل المقطع العرضي للفايبر على الشكل D. تم اختبار هذا المتحسس على محلول ملح كلوريد الصوديوم بمعامل انكسار يتراوح من 1.333 الى 1.363. ثم تم طلاء المتحسس بجزيئات الذهب النانوية بسمك 20 nm وتم اختباره على نفس محلول ملح كلوريد الصوديوم. ثم تم طلاءه بجزيئات الذهب النانوية بسمك 30 nm للحصول على اعلى حساسية تبلغ 466.66 nm/RIU